

# Simulation Study on the Adsorption Properties of Linear Alkanes on Closed Nanotube Bundles

James J. Cannon,<sup>\*,†</sup> Thijs J. H. Vlugt,<sup>‡</sup> David Dubbeldam,<sup>§</sup> Shigeo Maruyama,<sup>†</sup> and Junichiro Shiomi<sup>\*,†,||</sup>

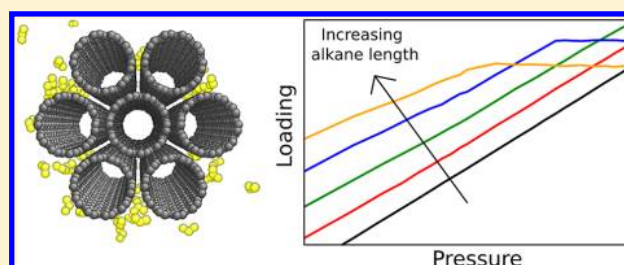
<sup>†</sup>Department of Mechanical Engineering, The University of Tokyo, 7-3-1 Hongo, Bunkyo-ku, Tokyo 113-8656, Japan

<sup>‡</sup>Process & Energy Laboratory, Process & Energy Department, Delft University of Technology, Leeghwaterstraat 44, 2628 CA Delft, The Netherlands

<sup>§</sup>Van 't Hoff Institute for Molecular Sciences, University of Amsterdam, Science Park 904, 1098 XH Amsterdam, The Netherlands

<sup>||</sup>Japan Science and Technology Agency, CREST, Chiyoda, Tokyo 102-0075, Japan

**ABSTRACT:** Adsorption onto carbon nanotube bundles may find use in various applications such as gas preconcentration and separation, and as a result, it is of great interest to study the adsorption properties of such bundles. The adsorption of linear alkanes, with their systematic variation through chain length, is particularly useful to explore the effects of molecular length on adsorption characteristics. We have conducted grand-canonical Monte Carlo simulations of light linear alkanes adsorbing onto closed nanotube bundles to explore these effects in a systematic manner. Our results demonstrate how adsorption into the grooves of the bundle is favored with alignment of the alkanes along the nanotube axis. We describe in detail the effects of competition for adsorption in the grooves and on the bundle as a whole, and highlight how selectivity can be tuned through careful choice of pressure and temperature. Finally, we describe how it is possible to derive a systematic relation between the length of the alkane and its loading on the bundle, and discuss its usefulness in applying ideal adsorbed solution theory (IAST) to predicting competitive mixed adsorption over a wide range of pressures. We also focus in turn on the ability of IAST to capture adsorption–saturation effects.



## INTRODUCTION

There is great interest in using carbon nanotubes for applications such as molecular sensors<sup>1,2</sup> or as preconcentrators<sup>3</sup> because their large area-to-mass ratio offers a significant number of potential adsorption sites. Such a large number of potential sites promotes strong interaction between the molecules and the nanotubes, with subsequent positive implications for the desired measurement or effect. Rather than being isolated in nature, however, nanotubes almost always form bundles, and this alters the adsorption of molecules compared with isolated nanotubes. Whereas such isolated nanotubes would offer completely isotropic adsorption around the cylindrical axis, the presence of a number of different adsorption sites in the bundle makes the adsorption cylindrically anisotropic (Figure 1). In addition, the greater number of close-range carbon atoms surrounding a pore increases interaction with the gas molecules and enhances the adsorption beyond that of an isolated carbon surface.<sup>4,5</sup> Because each type of adsorption site has slightly different adsorption strength and confinement characteristics, each site can be expected to display its own unique adsorption properties, which could be exploited for application purposes.

Nanotube bundles have long been of interest for adsorption applications, and early studies focused on the characterization of the bundle pores to understand more about their properties and influence on adsorption. For example, small molecules, able

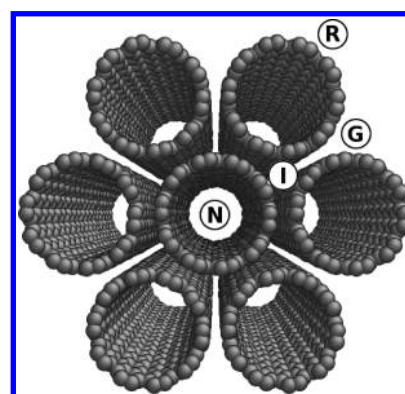


**Figure 1.** Four-principle adsorption sites of a hexagonal nanotube bundle consist of inner-nanotube sites (N), interstitial sites (I), groove sites (G), and ridge sites (R).

to penetrate into even the small interstitial pores, have been used to explore adsorption characteristics on both an experimental and a theoretical basis.<sup>6–10</sup> Among other things, this highlights the enhanced adsorption that arises due to the

**Received:** April 23, 2012

**Revised:** July 5, 2012

**Published:** July 5, 2012

presence of the pores. Furthermore, the nature of the adsorption has been shown to be unusual, with “1D” alignment of molecules within the grooves of the bundle.<sup>11–13</sup> A number of characterization studies have also been conducted with gases such as methane at low temperature<sup>14–16</sup> with the low temperatures accentuating the effects on adsorption by the different sites.

The study of alkane and alkene adsorption onto bundles has become of increasing interest to examine the selectivity of nanotube bundles in a systematic fashion. Because alkanes interact with the carbon atoms of nanotubes through the relatively simple van der Waals (VDW) interactions, and because linear alkanes differ only by the length of their carbon chain, such alkanes offer clear insight into the effects of molecular length on adsorption in bundles. As a result, during recent years, a number of studies have considered such adsorption, particularly using molecular simulation, because this offers clear detail about the location and energies of molecular adsorption. For example, adsorption of pure alkanes and competitive adsorption of mixed alkanes have been examined, showing how inside the bundle large alkanes can be replaced by small alkanes at high pressure due to entropic effects.<sup>17</sup> In general, however, where competition between species is negligible (e.g., at low pressures), larger alkanes adsorb more strongly than smaller alkanes due to their greater VDW interaction.<sup>18</sup> When considering the outer surface of the bundle, such adsorption occurs more strongly in the grooves if they are accessible compared with the ridges of the bundle,<sup>4,5</sup> although the strongest adsorption of alkanes over the whole bundle occurs inside the nanotubes themselves if they are open and accessible.<sup>19,20</sup> Further comparisons of adsorption between alkanes and their corresponding alkenes have highlighted the sensitivity of such pores, allowing differences in adsorption characteristics to be generated simply by the saturation (or lack thereof) of molecular bonds.<sup>21,22</sup>

Whereas a number of theoretical studies have offered valuable information about the internal adsorption characteristics by considering infinitely periodic bundle systems (considering inner-nanotube and interstitial sites only),<sup>17,23</sup> a number of studies have highlighted that inclusion of the outer surface of the bundle in simulations greatly assists in obtaining closer agreement with experiment and that this can be important when considering competition between different adsorbing species.<sup>24–28</sup> When growing nanotubes in the form of mats or films, for example, the sparse nature of the nanotubes will cause them to form isolated bundles,<sup>29</sup> and therefore the outer surface of these bundles plays a deciding role in the adsorption characteristics. As a result, to enhance the realism of simulations, it is important to include this outer surface. Furthermore, in an aim to obtain greater correlation between simulation and experiment, some authors have shown that the simulation of a heterogeneous range of nanotube diameters within the bundle (resulting in nonideal packing of the nanotubes and subsequently larger interstitial pores)<sup>14,15,30</sup> as well as assuming some of the nanotubes are open<sup>31</sup> can be helpful in improving agreement between simulation and experiment. It can in many cases, however, be preferable to have completely closed nanotubes because the process of oxidation that leads to the opening usually introduces unwanted defects. As a result, the “N” sites in Figure 1 are often inaccessible to the adsorbing molecules.

When considering the adsorption of molecules such as alkanes onto bundles of small closed nanotubes, surface effects

will dominate the adsorption and selectivity. Whereas it is clear that alkanes will generally favor groove sites, it is not yet clear to what extent this can be used to separate similar molecules such as alkanes. Furthermore, it is of interest to consider what quantitative relation there is between the adsorption of the alkanes and their chain length in a realistic system and to examine to what extent prediction of mixed adsorption is possible. To investigate these issues, we have conducted grand-canonical Monte Carlo (GCMC) simulations of pure and mixed adsorption of small alkanes onto closed nanotube bundles and have examined the nature of the adsorption as well as the potential for selectivity and the predictability of such results.

This article is organized as follows: After detailing the simulation system, we describe the adsorption characteristics of the alkanes onto the nanotube bundle, both in terms of pure alkanes and in terms of alkane mixtures competing for adsorption. We then turn to the predictability of the adsorption of pure and mixed alkanes before making a summary of the results.

## SIMULATION DETAILS

Adsorption of linear alkanes from methane to hexane have been considered ( $C_nH_{2n+2}$ , where  $n = 1\ldots6$ , referred to in an abbreviated form of “ $C_n$ ” throughout this paper) using GCMC simulations. The system is prepared in the following way: A nanotube bundle consisting of seven nanotubes is prepared in the formation shown previously in Figure 1. Each nanotube is a (10,10) armchair nanotube and is 13.56 Å in diameter. Separation between the nanotubes is set so that the minimum distance corresponds to the VDW radius of 3.21 Å for carbon–carbon interactions (taken from the work of Werder et al.<sup>32</sup>). This study will therefore represent results for a bundle in a tightest-packing scenario. Furthermore, whereas the bundle is the tightest possible configuration, the results should hold for larger bundles, too, because the size and shape of the pores will not change significantly. The carbon atoms are fixed in position for all simulations because framework flexibility has been shown, in general, to have a minor influence on adsorption.<sup>33</sup> Using periodic boundary conditions, the nanotubes are essentially infinite in length, and the interior of the nanotubes (“N” sites in Figure 1) is blocked to molecular adsorption to reproduce the realistic condition of an unopened bundle. The presence of periodic boundary conditions also prevents any adverse finite-size effects. A system length of 44 Å is used because it represents a system that is statistically sufficient (no difference in results is observed when the length is doubled) while maintaining reasonable computational cost. Because the interest is in an isolated bundle, the Cartesian axes perpendicular to the direction of the bundle are ~85 Å in length, giving ~50 Å between periodic images. This is sufficient for the bundle to be considered isolated and allows examination of surface adsorption. The TraPPE-UA potentials are used to describe the interaction between the alkanes,<sup>34</sup> which treat the molecules flexibly, combining hydrogen atoms with their corresponding carbon atoms to form a chain of single-site pseudoatoms. Lorentz–Berthelot combining rules<sup>35</sup> are meanwhile used for nonbonded heterogeneous atomic interaction.

For a given simulation, the reservoir surrounding the system is at constant temperature, pressure, and chemical potential. As with any GCMC simulation, the probability of accepting an insertion of a molecule into the system depends on both the parameters of the coupled bath and the energy of the proposed

insertion location in the system. Any insertion attempts inside the nanotubes are rejected through an applied blocking potential because they are considered to be closed. For the insertion of the alkane chains, the configurational-bias Monte Carlo (CBMC) method is used.<sup>34</sup> In addition to insertion and deletion trial moves, translation and rotation trial moves are also permitted as well as regrowths of the molecules. In addition to complete regrowths, the regrowths can also be partial, in which case only part of the molecule undergoes regrowth trials, reproducing internal degrees of freedom. Each simulation consists of 20 000 initialization cycles and then 20 000 measurement cycles. Each cycle consists of a number of trial moves equal to the number of alkane molecules in the system (with a minimum of 20 moves), so on average, each cycle will see each molecule attempt one trial move. To establish an isotherm, adsorption is measured for a given temperature over a range of pressures, from 0.01 kPa to 1000 kPa for methane ("C1") and ethane ("C2"), and up to the pressure at which saturation occurs for propane ("C3") and larger molecules. Tests reveal no hysteresis, and therefore calculations at the various pressures can be run in parallel.

To enhance further the realism of the simulations, gases are not assumed to be ideal; that is, the pressure is not equal to the fugacity. This requires knowledge of the relation between chemical potential (or fugacity) and pressure, which is achieved through the Redlich–Kwong equation of state.<sup>36</sup> For the simulation of alkane mixtures, the Lewis and Randall rule<sup>37</sup> is used to calculate the chemical potential (or fugacity) of each species in the mixture at the given pressure. For further details of the simulation method, the reader is referred to papers by Dubbeldam et al.<sup>38</sup> and Vlucht et al.<sup>39</sup>

## RESULTS AND DISCUSSION

**Adsorption of Pure and Mixed Alkanes.** Figure 2 shows how the pure alkane adsorption varies with alkane length and

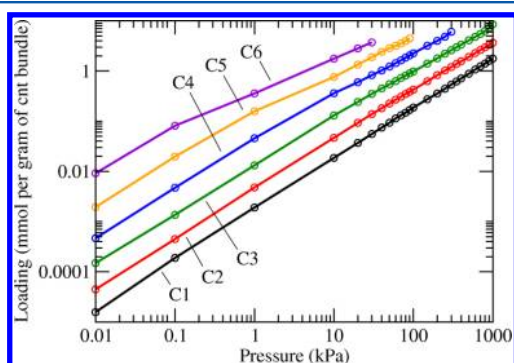


**Figure 2.** Adsorption of each pure alkane onto the nanotube bundle, from methane ("C1") to hexane ("C6"), at 300 K. The strongest adsorption can be observed for the largest alkane.

pressure at 300 K. As expected, a longer alkane results in greater adsorption, arising because the greater number of carbon atoms in a given alkane chain induces a stronger VDW interaction. Although a blocking potential is not applied to the interstitial pores as it is inside the nanotubes, their small size is observed to permit no adsorption, and so all adsorption here is on the surface of the bundle. The linear shape of the isotherm is consistent with other surface studies of light molecules<sup>19</sup> although interestingly of marked contrast with the type V isotherms that arise when adsorption inside the nanotubes is

permitted,<sup>17</sup> with sudden filling occurring over a short pressure range, preceded and followed by a slow increase in adsorption with pressure. This highlights how the form of the isotherms can give valuable information regarding the nature of adsorption by the bundle. Furthermore, in contrast with previous experimental studies of low-temperature methane adsorption where distinctive stages of adsorption could be observed due to the presence of the groove, here no inflection points are observed, and the adsorption is quite linear; a result of the higher temperature. Whereas the lack of experimental data limits comprehensive comparison of these results to experiment, the general increase in adsorption strength with alkane length is consistent with the trend observed in experiment.<sup>20</sup>

To examine the ability of the bundle to separate alkanes, we considered a mixture of alkanes, C1 to C5. The composition of the molecules in the gas phase is in the ratio 5:4:3:2:1 for C1 to C5, respectively (i.e., the composition is at approximately equal mass ratio). Figure 3 demonstrates how, at low loading, larger

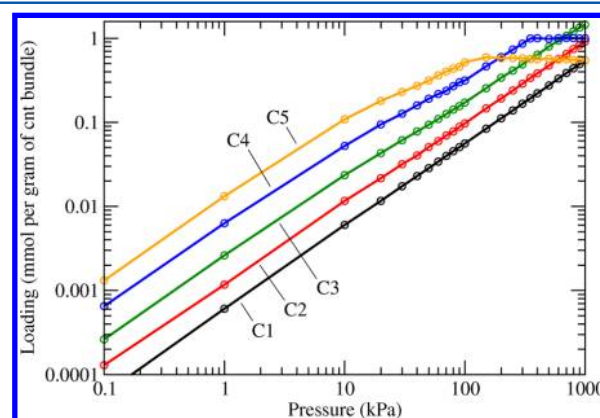


**Figure 3.** Adsorption of an equi-mass mixture of alkanes at 300 K from methane ("C1") to pentane ("C5"). At lower pressures, as in the case of pure alkanes, the larger alkanes adsorb more strongly, but saturation of large alkanes at higher pressures begins to reverse this trend.

alkanes adsorb more strongly. At high pressures, because larger alkanes have lower saturation pressures, a change in the ratio of the loading occurs. Furthermore, there is no evidence of hysteresis as our tests indicate that a sudden increase to the prescribed pressure and a gradual increase give the same results.

To isolate the effects of the grooves, the same mixed adsorption isotherm is calculated for a single (35,35) armchair nanotube of similar diameter and surface area to the bundle. Comparing the adsorption of C2–C5 against that for C1 (Figure 4), the presence of the grooves can be seen to increase the selectivity between the alkanes at lower pressures, whereas at higher pressures there is no difference in the relative adsorption. The grooves assist selectivity at lower pressures because they are filled preferentially by the stronger-interacting larger molecules at the expense of the weaker-interacting smaller molecules, forcing them to adsorb onto outer sites that also have weaker adsorption properties than the grooves. At higher pressure, there is greater overall adsorption, which negates the special nature of the grooves as competition for all sites increases and leads to no difference in selectivity between the bundle and the large single nanotube. The saturation of the larger alkanes at high pressures acts to reduce the rate of increase in adsorption with pressure and when combined with competition for space, and entropic effects within the grooves



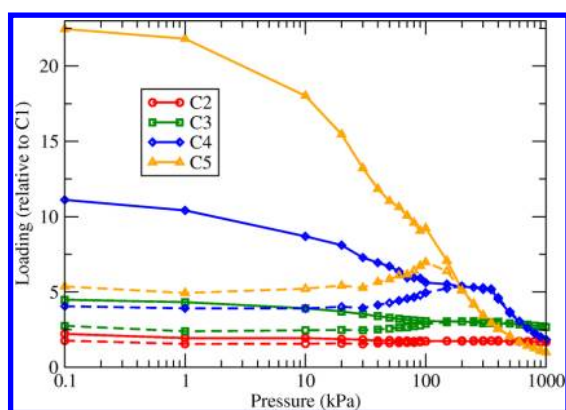


**Figure 4.** Adsorption of C2 to C5 relative to C1 for the bundle (solid lines) and a smooth large nanotube (dashed lines) with a diameter and surface area similar to that of the bundle. The presence of the grooves can be seen to increase the selectivity at lower pressures.

can result in a decrease in the amount of adsorption, as demonstrated for C5 in Figure 5. This reduction is shown

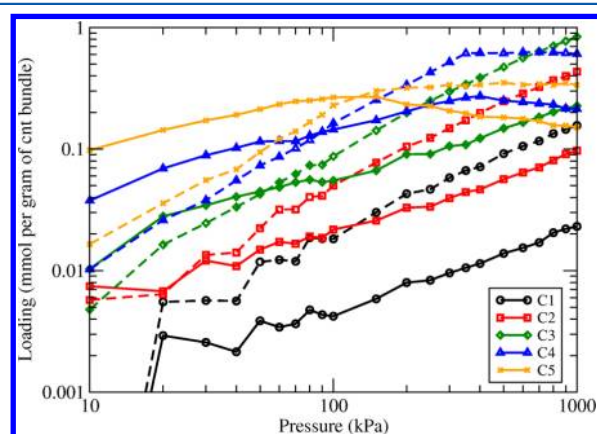


**Figure 5.** Average loading of molecules inside the grooves (solid lines) and immediately outside the nanotube bundle (dashed lines) in the C1–C5 equi-mass alkane mixture. Adsorption saturation of C4 and C5 is observed in correspondence with that shown in Figure 3. Replacement of the large alkanes inside the grooves is also observed at high pressures.

particularly clearly when considering the change in the radial density of the alkanes between 100 kPa and 300 kPa (Figure 6), with a decrease in the loading of C5 inside the grooves accompanied by a reduced increase outside.

As competition for adsorption sites becomes greater, one might expect compression effects to reduce the end-to-end length of the alkanes; however, this is not the case; the length remains constant at all pressures (not shown here). The angle of the alkanes relative to the nanotube axis is, however, very much dictated by the presence of the grooves, as is shown for the alignment of C5 (pentane) at 100 kPa in the mixed solution (Figure 7). As could be expected, alkanes are strongly aligned with the nanotubes at the base of the groove, and as molecules are positioned further out of the grooves, the orientation becomes progressively more random. Interestingly, just beyond the mouth of the groove (just beyond a distance of 0 Å in Figure 7), moderate promotion of aligned orientation occurs again, corresponding to the alignment of alkanes side-by-side. The induced alignment then becomes weaker as the distance outside the bundle increases further.

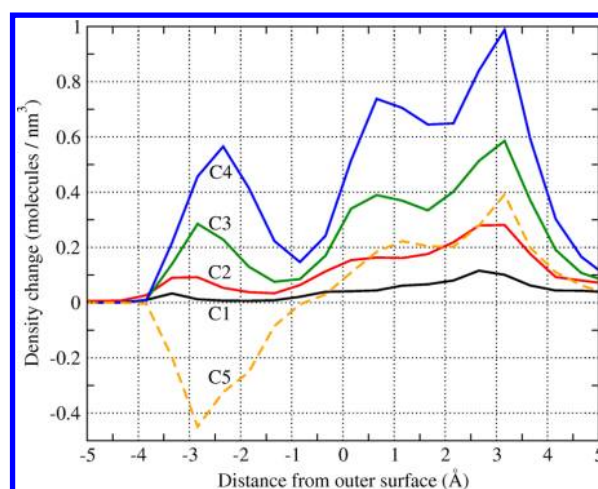


**Figure 6.** Difference in average radial density between 100 and 300 kPa for the C1–C5 alkane equi-mass mixture. A positive value indicates an increase in density with pressure. The increase in C5 is much reduced due to its reaching saturation pressure. When this is combined with competition for space and entropic effects within the grooves, this results in a decrease in the amount of C5, whereas other alkanes continue to experience an increase. Zero on the  $x$  axis is the outer edge of the bundle (as in the inset of Figure 7), so a negative position corresponds to a location in the groove.

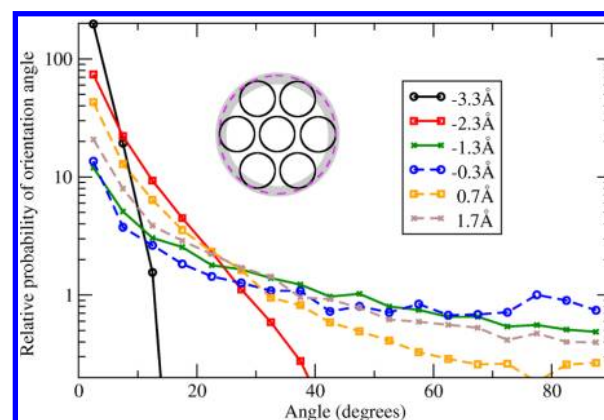


**Figure 7.** Orientation of C5 (pentane) molecules in the C1–C5 equi-mass mixture at 300 K and 100 kPa for given distances from the edge of the bundle. The edge is marked in the inset schematic with a dashed line, and the range of distances (−3.3 to 1.7 Å) are indicated by the shaded region. Therefore, a negative position corresponds to a position inside the groove. An angle of 0° corresponds to alignment with the nanotube axis, whereas that of 90° corresponds to cross-orientation. The relative probability of the orientation angle is calculated by taking the observed probability derived from simulation snapshots and dividing it by the probability that would be expected if the orientation was completely random. Therefore, a relative probability greater than 1 corresponds to an increased probability of that orientation occurring. Each angle is split into 5° bins for statistical analysis.

The adsorption of the alkanes onto the bundle occurs because the thermal energy is not sufficient to escape the VDW attraction to the carbon atoms of the nanotubes. By reducing the temperature, the thermal energy is reduced, and hence more adsorption is expected. What is interesting to consider is how this effects the adsorption characteristics in contrast with those already observed at 300 K. Comparing the properties at 100 kPa and 300 kPa again, Figure 8 shows the dramatic effect

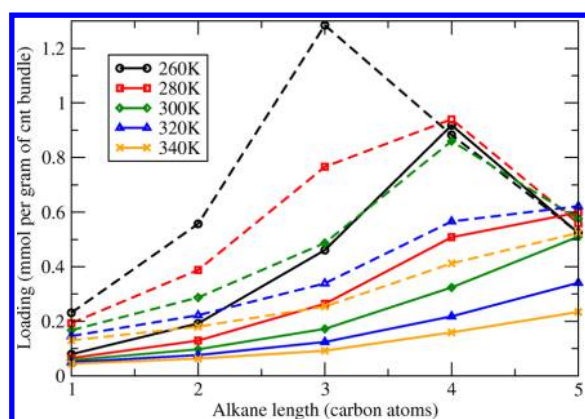


**Figure 8.** Influence of temperature on bundle loading for a C1–C5 equi-mass alkane mixture. Solid lines are at 100 kPa, whereas dashed lines are at 300 kPa.

that temperature can have on the adsorption-selectivity of the bundle. Whereas the previous results at 300 K showed C5 being replaced by smaller molecules, at 340 K, the order in loading from C1 to C5 is restored. At lower temperature, however, the opposite is true; at 260 K, not only C5 but also C4 experiences saturation, leaving C3 with the greatest loading. This demonstrates clearly that by careful cycling of both temperature and pressure, it is possible to adsorb selectively chosen alkanes.

#### Predictability of Alkane Adsorption. Pure Adsorption.

As previously mentioned, one motivation for the study of alkane adsorption is that each alkane differs in a systematic manner from the next (i.e., by the simple addition of carbon atoms). As a result, it allows study of the adsorption in a methodical manner and may allow a relation to be derived between the length of the alkane and its adsorption characteristics. We have therefore examined the predictability of the loading of pure alkanes onto the nanotube bundle as a function of the alkane length. This has been performed both at 300 K and at the lower temperature of 260 K to examine the effects of temperature, too. Isotherms for pure alkanes were shown previously in Figure 2 for 300 K, and in this style a best-fit line can be applied to reproduce this data for each pure alkane at each temperature. Not only can this be done for loading as a function of pressure, as in the case of Figure 2, but it can also be done as a function of fugacity in a similar manner.

In fact, for the current purposes of predicting pure alkane adsorption, there is a clear advantage to predicting this in terms of fugacity rather than pressure. This is because that unlike at 300 K, where the number of molecules becomes computationally expensive as the phase changes and the free space around the bundle is filled, the loading of pure molecules such as C4 and C5 at 260 K saturates only in the local volume around the bundle. Because the molecules do not fill the free space away from the bundle, it is clear that the bundle is required for favorable adsorption at this temperature. If one assumes that the gas is ideal (i.e., fugacity = pressure), as is done in some works,<sup>40,41</sup> then it is impossible to apply a simple isotherm to describe the loading with pressure because such a simple description cannot capture the leveling-off of the loading at 260 K during saturation. If one treats the gas as nonideal, however, then even as the loading as a function of pressure saturates, the loading as a function of fugacity does not, and therefore a simple isotherm is sufficient to describe the adsorption over the full range of fugacity, which can then subsequently be converted back to pressure. For this reason, pure adsorption predictability is studied in terms of fugacity.

A number of isotherm forms exist for the description of loading versus pressure or fugacity at constant temperature; however, two that combine simplicity with accuracy are the Langmuir isotherm<sup>42</sup> of the form  $n = (n_s k_f) / (1 + k_f)$  and the Freundlich isotherm<sup>43</sup> of the form  $n = a f^b$ , where  $n$  is the number of adsorbates,  $f$  is the fugacity,  $n_s$  is the saturation loading, and  $k$ ,  $a$ , and  $b$  are constants. Note that for the relations to be thermodynamically correct  $n$  needs to be proportional to  $f$  at low pressure, and so strong deviation of the value of  $b$  from unity in the Freundlich isotherm is undesired. Of the two isotherms, the Freundlich isotherm proved to fit the data most accurately. Because the Langmuir isotherm is developed based on the principle of a single site, it was considered whether this could be improved by a double-langmuir isotherm to represent two sites; however, this led to no improvement of the fit. A double-Freundlich isotherm meanwhile produced only a marginal improvement in the already-good fit, at a cost of doubling the number of variables, and was therefore disregarded.

Each alkane isotherm can be described in the form of a Freundlich isotherm,  $n = a f^b$ , with correlation coefficients between the predicted and actual data of  $R^2 = 0.999$  or higher for all alkanes. The values of  $a$  and  $b$  as a function of alkane

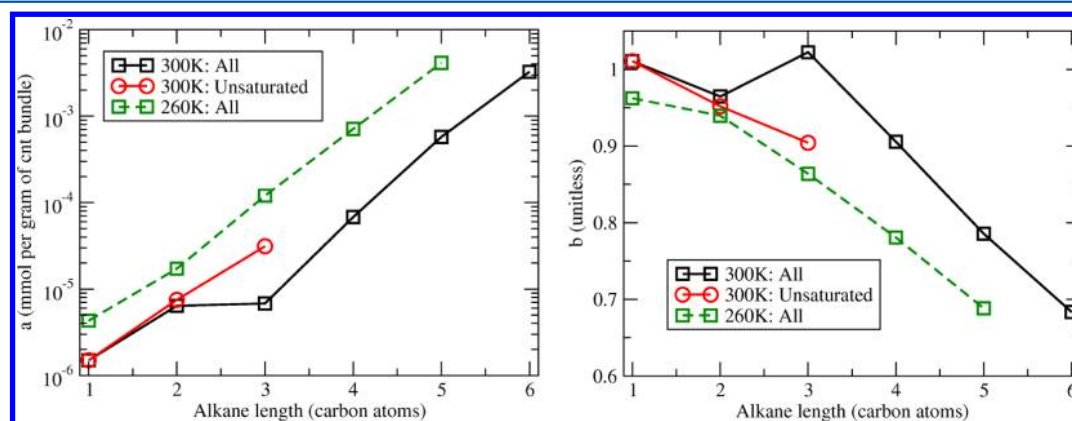


**Figure 9.** Variation of the value of constant  $a$  (left) and  $b$  (right) within the Freundlich-isotherm fit  $n = F^b$  describing pure-alkane adsorption. “All” corresponds to  $a$  and  $b$  values derived from a fit over all data, whereas “Unsaturated” corresponds to fits based only on lower pressures, where complete filling (saturation) of the grooves has not yet occurred. (See the main text for more details.)

length (number of carbon atoms), fitted over all pressures, are shown for both temperatures in Figure 9. The variation of these constants can be described by exponential functions  $a = j_1 j_2^{n_c}$  and  $b = j_3 j_4^{n_c}$ , where  $n_c$  is the number of carbon atoms in the alkane chain and  $j_{1,4}$  are constants. The values of the constants for 300 K are found to be  $j_1 = 1.99 \times 10^{-7}$  Pa,  $j_2 = 4.71$ ,  $j_3 = 1.16$ , and  $j_4 = 0.93$ , whereas for 260 K the values are  $j_1 = 6.44 \times 10^{-7}$  Pa,  $j_2 = 5.73$ ,  $j_3 = 1.09$ , and  $j_4 = 0.92$  for a final equation of the form

$$n = (j_1 j_2^{n_c}) f(j_3 j_4^{n_c}) \quad (1)$$

Whereas the increase in the values of  $a$  and  $b$  is largely smooth at 260 K, this is not the case at 300 K. The trend for C1 and C2 seems out of line with the trend observed for all of the larger alkanes; there is a discontinuity between C2 and C3. It can be considered that the value of  $a$  in the Freundlich isotherm is essentially the gradient of the loading with fugacity (so a larger value leads to a greater increase in loading per unit of fugacity-increase), and the value of  $b$  describes the curve of the gradient (so a value greater than 1 describes a curve upward, whereas a value less than 1 describes a more asymptotic trend of loading with fugacity). If the trend of  $a$  for alkanes C3 to C6 at 300 K is extrapolated back for C2 and C1 in Figure 9, then C1 and C2 can be seen to have larger-than-expected values of  $a$ : they have a stronger increase in adsorption with fugacity than expected. Similar extrapolation for  $b$  meanwhile shows that C1 and C2 have a lower value of  $b$  than would otherwise be expected: in other words, they display slightly sharper asymptotic behavior than expected.

Figure 10 shows how the adsorption into the grooves for C1 and most of C2 is linear (nonsaturating), whereas C3 and

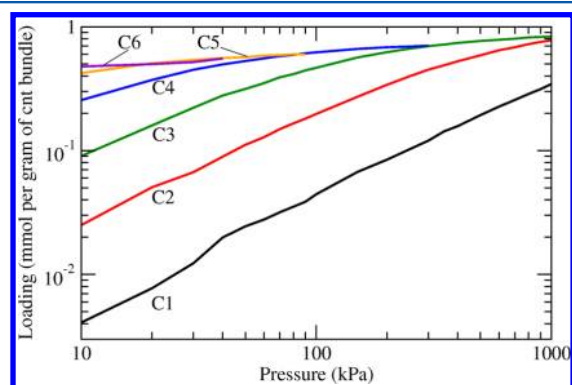


**Figure 10.** Loading of molecules in the grooves of the bundle for pure-alkane adsorption at 300 K.

longer alkanes experience clear saturation of adsorption in the grooves during the pressure-range investigated here. This corresponds well with the notion that C1 and C2 experience a stronger adsorption increase per unit of fugacity-increase than would otherwise be expected because the adsorption into the grooves is more favorable than that outside the grooves. Furthermore, although the curve for C1 and C2 is almost straight (giving a value of  $b$  near unity), the fact that  $b$  is slightly lower than would be expected is consistent with minor saturation in the confined grooves compared with the freer adsorption outside the grooves.

To confirm the role of the grooves in the inflection in  $a$  and  $b$  at 300 K, one can calibrate the Freundlich isotherm for larger alkanes using only lower pressures before complete filling of the

grooves occurs. For C1, this corresponds to pressures up to 1000 kPa (i.e., all pressures considered in this study), for C2, this is up to 300 kPa, and for C3, this is up to just 40 kPa. For alkanes C4 and larger, groove-saturation occurs for even very low pressures; therefore, only C1 to C3 are considered. The values for  $a$  and  $b$  derived from these lower pressures are also shown in Figure 9, demonstrating clearly how the inflection point in the trend now disappears. This demonstrates conclusively that the presence of the grooves of the bundle has an important impact in enhancing adsorption of the smallest molecules.

The trend in the values of  $a$  and  $b$  at 260 K meanwhile can be understood to simply be an extension of these effects. It has been highlighted how alkanes at 260 K adsorb more strongly onto the bundle, and this is reflected in the value of  $a$ , which sees an increase in value for all alkanes. Greater asymptotic behavior is meanwhile suggested by the decrease in value of  $b$ , consistent with the requirement of the presence of the bundle for adsorption into the system and the resulting reduction in freedom of the molecules to adsorb elsewhere within the system. The slight inflection observed for C1 at this temperature arises as a result of greater groove-based adsorption over the range of pressures studied compared with the larger alkanes.

**Mixed Adsorption.** Beyond prediction of pure-alkane isotherms, it is of interest to extend the models developed for pure adsorption to predict the adsorption characteristics of mixed alkanes. The advantage of such predictability is that only individual pure adsorption isotherms are required, and then any combination of alkanes at the given temperature can be calculated. For the purpose of predicting mixed adsorption isotherms based on pure isotherms, ideal adsorbed solution theory (IAST) is often used and has been shown to hold for a wide range of different absorption situations, such as in hydrogen isotope separation using nanotubes,<sup>44</sup> CO<sub>2</sub> separation from N<sub>2</sub> for environmental applications using metal–organic frameworks (MOFs),<sup>45</sup> and ethane separation from a mixture of natural gas,<sup>46</sup> to name a few. The background to IAST and its derivation is well-detailed in the original work<sup>47</sup> as well as those more recent.<sup>40,48</sup>

Obtaining the pure adsorption data for the purposes of predicting the mixed adsorption can be achieved through either experiment or simulation at the desired temperature and pressure. It can be observed from Figure 2, however, that at 300 K pure adsorption data are limited because beyond a certain pressure phase change and complete filling of the simulation cell occurs. The limit for mixed adsorption is much higher, however (Figure 3), because complete filling of the simulation cell by individual species does not occur. This is where the  $n = af^b$  models derived in the previous section for pure alkane adsorption are particularly useful: by extending the model for pure adsorption to higher pressures, we are able to predict mixed adsorption beyond the limit of pure adsorption data.

Figure 11 shows the predictive ability of IAST for the adsorption of a C1–C5 alkane mixture on the nanotube bundle at both 260 and 300 K. Close agreement is generally observed between the predicted and measured isotherms for the mixture. Furthermore, the saturation in the adsorption is also captured well by IAST, showing the wide range of applicability of IAST to various situations. Deviation in the accuracy of IAST in reproducing the mixed adsorption isotherm stems from small deviations in describing the pure loading through the Freundlich isotherm; agreement could therefore be improved



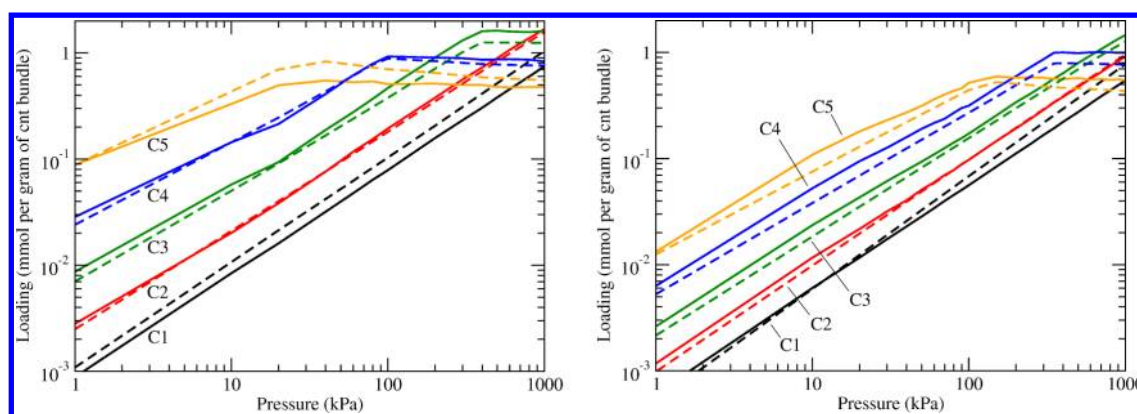


**Figure 11.** Actual adsorption isotherms (solid lines) for a C1–C5 mixture and the corresponding isotherms predicted through IAST (dashed lines) for 260 K (left) and 300 K (right) based on the pure adsorption models developed in the previous section.

with more accurate prediction of the pure-component isotherms.

## CONCLUSIONS

The adsorption of small linear alkanes onto a closed nanotube bundle has been studied using GCMC simulations. The adsorption of pure alkanes has been shown to be well-described by Freundlich isotherms, whereas selectivity of alkanes in a mixture has shown to be possible through careful choice of temperature and pressure, utilizing differing saturation pressures of alkane species. The grooves of the bundle have been shown to play an important role in enhancing selectivity at lower pressures, whereas at higher pressures the grooves become less important because confinement is experienced at all sites. The replacement of larger alkanes by smaller alkanes at high pressures, particularly in the grooves, has also been discussed. In general, adsorption has been shown to favor the grooves of the bundle strongly, and alkanes have been shown to promote alignment with the bundle deep in the groove and, less expectedly, at the mouth to the groove, too.

The predictability of adsorption has also been discussed for both pure and mixed alkanes. The adsorption of pure alkanes with fugacity has been shown to be quantitatively predictable through the number of carbon atoms,  $n_c$ , in the form  $n = (j_1 j_2^{n_c}) f(j_3 j_4^{n_c})$ , and this has helped highlight the enhanced adsorption at 300 K of methane and ethane arising through relatively high groove-saturation pressures. The applicability of IAST in predicting mixed alkane adsorption from pure isotherms has also been considered, showing close agreement with mixed-alkane simulations, including the capturing of adsorption-saturation as well as the competition for adsorption in the mixture. The usefulness in using pure-alkane models for the extension of IAST to higher pressures has been highlighted, and the importance of the accuracy of these pure isotherms for the predictive accuracy of IAST has also been discussed.

## AUTHOR INFORMATION

### Corresponding Author

\*E-mail: cannon@photon.t.u-tokyo.ac.jp; shiomi@photon.t.u-tokyo.ac.jp.

### Notes

The authors declare no competing financial interest.

## ACKNOWLEDGMENTS

This work is partially financially supported by the Japan Society for the Promotion of Science (JSPS, project 2200064) (J.C. and S.M.), the Japan Science and Technology Agency, CREST (J.S.), and a Grant-in-Aid for Scientific Research (22226006 and 19051016) (J.S. and S.M.).

## REFERENCES

- (1) Zhao, J. J.; Buldum, A.; Han, J.; Lu, J. P. *Nanotechnology* **2002**, *13*, 195–200.
- (2) Hong, S. Y.; Tobias, G.; Ballesteros, B.; El Oualid, F.; Errey, J. C.; Doores, K. J.; Kirkland, A. I.; Nellist, P. D.; Malcolm, L. H.; Davis, B. G. *J. Am. Chem. Soc.* **2007**, *129*, 10966–10967.
- (3) Hussain, C. M.; Mitra, S. *Anal. Bioanal. Chem.* **2011**, *399*, 75–89.
- (4) Rawat, D. S.; Furuhashi, T.; Migone, A. D. *Langmuir* **2009**, *25*, 973–976.
- (5) Cruz, F. J. A. L.; Mota, J. P. B. *Phys. Rev. B* **2009**, *79*, 165426.
- (6) Stan, G.; Crespi, V. H.; Cole, M. W.; Boninsegni, M. *J. Low Temp. Phys.* **1998**, *113*, 447–452.
- (7) Teizer, W.; Hallock, R. B.; Dujardin, E.; Ebbesen, T. W. *Phys. Rev. Lett.* **1999**, *82*, 5305–5308.
- (8) Williams, K. A.; Eklund, P. C. *Chem. Phys. Lett.* **2000**, *320*, 352–358.
- (9) Stan, G.; Bojan, M. J.; Curtarolo, S.; Gatica, S. M.; Cole, M. W. *Phys. Rev. B* **2000**, *62*, 2173–2180.
- (10) Simonyan, V. V.; Johnson, J. K.; Kuznetsova, A.; Yates, J. T. *J. Chem. Phys.* **2001**, *114*, 4180–4185.
- (11) Gatica, S. M.; Bojan, M. J.; Stan, G.; Cole, M. W. *J. Chem. Phys.* **2001**, *114*, 3765–3769.
- (12) Talapatra, S.; Migone, A. D. *Phys. Rev. Lett.* **2001**, *87*, 206106.
- (13) Calbi, M. M.; Cole, M. W. *Phys. Rev. B* **2002**, *66*, 115413.
- (14) Talapatra, S.; Migone, A. D. *Phys. Rev. B* **2002**, *65*, 045416.
- (15) Johnson, M. R.; Rols, S.; Wass, P.; Muris, M.; Bienfait, M.; Zeppenfeld, P.; Dupont-Pavlovsky, N. *Chem. Phys.* **2003**, *293*, 217–230.
- (16) Bienfait, M.; Zeppenfeld, P.; Dupont-Pavlovsky, N.; Muris, M.; Johnson, M. R.; Wilson, T.; DePies, M.; Vilches, O. E. *Phys. Rev. B* **2004**, *70*, 035410.
- (17) Jiang, J. W.; Sandler, S. I.; Schenk, M.; Smit, B. *Phys. Rev. B* **2005**, *72*, 045447.
- (18) Rawat, D. S.; Furuhashi, T.; Migone, A. D. *J. Phys. Chem. C* **2010**, *114*, 20173–20177.
- (19) Cruz, F. J. A. L.; Esteves, I. A. A. C.; Mota, J. P. B.; Agnihotri, S.; Muller, E. A. *J. Nanosci. Nanotechnol.* **2010**, *10*, 2537–2546.
- (20) Kondratyuk, P.; Wang, Y.; Johnson, J. K.; Yates, J. T. *J. Phys. Chem. B* **2005**, *109*, 20999–21005.
- (21) Cruz, F. J. A. L.; Esteves, I. A. A. C.; Agnihotri, S.; Mota, J. P. B. *J. Phys. Chem. C* **2011**, *115*, 2622–2629.
- (22) Jakobtorweihen, S.; Keil, F. J. *Mol. Simul.* **2009**, *35*, 90–99.

- (23) Mahdizadeh, S. J.; Tayyari, S. F. *Theor. Chem. Acc.* **2011**, *128*, 231–240.
- (24) Jiang, J. W.; Sandler, S. I. *Phys. Rev. B* **2003**, *68*, 245412.
- (25) Jiang, J. W.; Sandler, S. I. *Langmuir* **2004**, *20*, 10910–10918.
- (26) Jiang, J. W.; Sandler, S. I. *Fluid Phase Equilib.* **2005**, *228*, 189–195.
- (27) Heroux, L.; Krungleviciute, V.; Calbi, M. M.; Migone, A. D. *J. Phys. Chem. B* **2006**, *110*, 12597–12602.
- (28) Esteves, I. A. A. C.; Cruz, F. J. A. L.; Muller, E. A.; Agnihotri, S.; Mota, J. P. B. *Carbon* **2009**, *47*, 948–956.
- (29) Einarsson, E.; Shiozawa, H.; Kramberger, C.; Rummeli, M. H.; Gruneis, A.; Pichler, T.; Maruyama, S. *J. Phys. Chem. C* **2007**, *111*, 17861–17864.
- (30) LaBrosse, M. R.; Johnson, J. K. *J. Phys. Chem. C* **2010**, *114*, 7602–7610.
- (31) LaBrosse, M. R.; Shi, W.; Johnson, J. K. *Langmuir* **2008**, *24*, 9430–9439.
- (32) Werder, T.; Walther, J. H.; Jaffe, R. L.; Halicioglu, T.; Koumoutsakos, P. *J. Phys. Chem. B* **2003**, *107*, 1345–1352.
- (33) Vlugt, T. J. H.; Schenk, M. *J. Phys. Chem. B* **2002**, *106*, 12757–12763.
- (34) Martin, M. G.; Siepmann, J. I. *J. Phys. Chem. B* **1999**, *103*, 4508–4517.
- (35) Allen, M. P.; Tildesley, D. *Computer Simulation of Liquids*; Clarendon Press: Oxford, U.K., 1987.
- (36) McQuarrie, D. A.; Simon, J. D. *Molecular Thermodynamics*; University Science Books: Sausalito, CA, 1999.
- (37) Smith, J. M.; van Ness, H. C.; Abbott, M. M. *Introduction to Chemical Engineering Thermodynamics*; McGraw-Hill: Boston, 2001.
- (38) Dubbeldam, D.; Calero, S.; Vlugt, T. J. H.; Krishna, R.; Maesen, T. L. M.; Smit, B. *J. Phys. Chem. B* **2004**, *108*, 12301–12313.
- (39) Vlugt, T. J. H.; Krishna, R.; Smit, B. *J. Phys. Chem. B* **1999**, *103*, 1102–1118.
- (40) Chen, J. H.; Loo, L. S.; Wang, K. *J. Chem. Eng. Data* **2011**, *56*, 1209–1212.
- (41) Krishna, R.; Paschek, D. *Phys. Chem. Chem. Phys.* **2001**, *3*, 453–462.
- (42) Langmuir, I. *J. Am. Chem. Soc.* **1918**, *40*, 1361–1403.
- (43) Freundlich, H. *Kapillarchemie*; Akademische verlagsgesellschaft m.b.h.: Wiesbaden, Germany, 1909.
- (44) Tanaka, H.; Miyahara, M. T. *J. Chem. Eng. Jpn.* **2011**, *44*, 355–363.
- (45) Mason, J. A.; Sumida, K.; Herm, Z. R.; Krishna, R.; Long, J. R. *Energy Environ. Sci.* **2011**, *4*, 3030–3040.
- (46) Magnowski, N. B. K.; Avila, A. M.; Lin, C. C. H.; Shi, M.; Kuznicki, S. M. *Chem. Eng. Sci.* **2011**, *66*, 1697–1701.
- (47) Myers, A. L.; Prausnitz, J. M. *AIChE J.* **1965**, *11*, 121–127.
- (48) Murthi, M.; Snurr, R. Q. *Langmuir* **2004**, *20*, 2489–2497.